1998

Numerical Simulation of Transient Jet Interaction on a Generic Supersonic Missile with Fins*

Houshang B. Ebrahimi†
Sverdrup Technology, Inc., AEDC Group
Arnold Engineering Development Center
Arnold Air Force Base, TN 37389

Abstract

The objective of this investigation is to evaluate the transient effects of a reaction control jet on the aerodynamic performance of a generic interceptor missile. Three-dimensional computations of the highly turbulent flow field produced by a pulsed, lateral-jet control thruster and the interaction of this jet with the supersonic free stream and missile boundary layer were completed for different altitudes and thruster conditions. A generic supersonic missile-interceptor configuration consisting of a long, slender body (L/D = 14.1) containing fixed dorsal and tail fins was used in this study. Parametric computational fluid dynamic (CFD) solutions were obtained at two altitudes of 64.5 kft (19.7 km) and 115 kft (35.1 km). Computation of the flow-field behaviors at each altitude were completed for the following assumptions: (1) steady-state conditions, lateral control jet turned off, (2) steady-state conditions, lateral control jet turned on, (3) transient transient jet startup simulation, and (4) transient jet shutdown simulation. A thermally perfect gas ($\gamma = 1.4$) was assumed for the Mach number 5 free stream and the Mach number 3 lateral jet. Vehicle forces and moments were obtained for each solution by integrating the surface pressures and viscous shear stresses computed on the missile surfaces. These results are applied to assess the influence of the jet interaction (JI) effects on the transient aerodynamic performance of the missile. The analysis indicates that strong transient influence is predicted in the integrated normal force and pitching moment. These effects may be influenced by the dorsal fin interaction with the jet interaction (JI) region.

Introduction

To complete its mission successfully, a missile defense interceptor must be highly maneuverable when it travels at supersonic or hypersonic speeds. Quick-response maneuverability, especially during the end-game phase of the interceptor's mission, is achieved by a rapid airframe response-time to the attitude control system. Surface-mounted, fast-reacting, lateral-jet control thrusters issuing at large angles relative to the interceptor's direction of flight offer an effective supplement to conventional aerodynamic control surfaces, producing the required response times and improving the missile's agility and maneuverability.

The mutual interference of the jet thruster exhaust with the supersonic free stream leads to thrust and moment amplifications due to high-pressure regions that form upstream of the jet on the missile surface. This high-pressure region is created by the shock structure that develops in the supersonic free stream in front of the jet. Large regions of separated flow created by the missile boundary-layer interactions with the shock cause the high-pressure area to increase in size. This effect amplifies the response of the divert jets. Effective exploitation of this effect can lead to improved effectiveness of the missile interceptor. These solutions demonstrate that CFD can be applied to acquire a more complete understanding of this behavior. Insight into this phenomenon is necessary because at some missile orientations and flow conditions, the mutual interference of the jet thruster flow field with the free stream leads to "deamplification" (i.e., negative effects). Therefore,

* The research reported herein was performed by the Arnold Engineering Development Center (AEDC), Air Force Materiel Command. Work and analysis for this research were performed by personnel of Sverdrup Technology, Inc., AEDC Group, technical services contractor for AEDC. Further reproduction is authorized to satisfy needs of the U. S. Government.

† Sverdrup Technology, Inc./AEDC Group, Arnold Engineering Develpoment Center, Arnold Air Force Base, TN.

an understanding of the controlling factors that produce thrust amplification, as well as those that produce thrust deamplification, is critical to developing a credible design basis for optimal missile performance. The CFD results from this investigation, complemented with ground simulations can be applied to understand and quantitatively assess this phenomenon. The JI phenomena are described in Refs. 1 and 2.

The CFD solutions completed for this investigation demonstrate the potential to numerically simulate complex, three-dimensional JI flow fields and assess the influence of the transient jet interaction effects on the aerodynamic performance of the missile. However, just as JI phenomena pose a challenge for ground-test simulations, it is a formidable area for numerical simulations as well. Numerically simulating the transient, lateral control jet thruster flow-field behavior as it merges and interacts with the supersonic free-stream flow is one of the most complex propulsion flow-field phenomena to be addressed using state-of-the-art CFD techniques. A numerical scheme applied to transient JI flow-field problems must include the capability to accurately resolve the complex shock structures and boundary-layer separation regions associated with such flows, and it also predicts the time-accurate characteristics of these highly vortical and possibly chemically reacting flows. (This study does not include chemical effects.)

Objectives

The objectives of this effort are:

1. To demonstrate the feasibility of CFD techniques to analyze JI flow transient behaviors and verify the utility of the solutions for interceptor missile design and development concepts.

2. To provide an extensive interrogation of computational flow-field results obtained at representative operational conditions. Detailed analyses of transient JI flow-field behaviors are not plausible from the limited ground test collections measuring forces and moments. The transient effects are limited by the response of the instrumentation, and spatial flow-field visualization of complex, time-accurate transient events has not been captured in ground simulations.

3. To computationally visualize and quantify the transient JI effects resulting from a pulsed, lateral-jet control thruster on the aerodynamic performance of a generic supersonic/hypersonic ballistic missile defense interceptor at representative operational conditions.

Approach

The approach consisted of a computational experiment of JI flow-field behaviors involving parametric CFD investigations of the computed flow fields and resulting forces and moments at two altitude conditions. The effects of the divert jet under transient startup and shutdown are evaluated, as well as steady-state JI behaviors. Steady-state solutions were also obtained when the divert thruster was present on the missile body, but not operating. The same missile and divert thruster geometries were assumed for all simulations. The generic missile geometry shown in Fig. 1 was provided by the John Hopkins University Applied Physics Laboratory. A generic long, slender missile body design including forward and aft fins was evaluated. This geometry is representative of interceptor designs and was selected because divert thruster transient effects are suspected to be potentially influenced by the presence of fins on the missile. The missile free-stream Mach number was maintained at Mach number 5.0. The Mach number at the exit of the diverging divert thruster's nozzle was nominally 3. A thermally perfect gas was assumed in the CFD approximation for the free stream and the divert flow. The ratio of specific

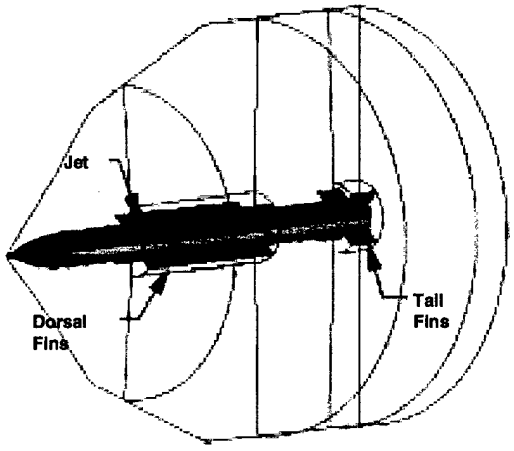

Fig. 1. Surface definition showing zonal decomposition.

heats (γ) equal to 1.4 was specified for the free stream and the divert jet flow. Three-dimensional, thermally perfect flow-field solutions were completed for the interceptor/divert motor flow-field interactions at two altitude conditions, 64.5 kft (19.7 km) and 115 kft (35.1 km). These missile flight conditions are representative of the actual operation scenario of the missile interceptor. The angle of attack of the interceptor was specified as 0.0 deg. The divert jet was maintained at the same position on the interceptor missile with its effluents situated at 90 deg to the thrust vector of the interceptor for all simulations.

The resulting CFD flow-field solutions are contrasted to determine the transient effects of divert thruster jet startup and shutdown behaviors. The flow field surrounding the interceptor missile body when the divert thrusters are present on the interceptor body, but not operating is also computed. Even when the divert jets are turned off, there is an influence on the missile body forces due to cavity flow created by the presence on the thruster opening on the body. This analysis was completed at two altitudes to determine the altitude effect, if any, on the interaction behavior and resulting missile body forces and moments.

The divert jet is located between two of the dorsal fins at the center of gravity for the interceptor missile. The divert jet thrust chamber consisted of a converging/ diverging nozzle geometry and stagnation conditions specified such that the nominal Mach number at the nozzle exit is 3.0. The divert jet flow was included in the computational domain. The stagnation conditions specified for the divert thrust are given below:

$$P_{oj} = 2590 \text{ psia } (176 \text{ atm})$$

$$T_{oj} = 4100^{\circ}\text{R } (2278 \text{ K})$$

The free-stream conditions for the two altitudes investigated at 19.7 km and 35.1 km are shown in Table 1.

The CFD solutions were designed to study the flow-field behaviors focusing on the transient effects on the forces and moments that result from the operation of a Mach 3.0 pulsed jet, located at the center of gravity on the interceptor missile and discharging perpendicular to the Mach 5 free-stream flow. The CFD investigation included four solutions at each of the altitudes mentioned above. The solutions comprised steady-state calculations with the divert thruster turned jet off and a steady-state solution with the jet on, as well as the transient startup of the jet and a transient shutdown of the jet. The eight CFD cases investigated are summarized in Table 2.

Table 1. Free-stream Conditions

Parameter	Altitude = 19.7 km (64.5 kft)	Altitude = 35.1 km (115 kft)
Flight Mach Number	5.0	5.0
Static Pressure, Pa (atm)	5833.7 (0.57)	558.2 Pa (0.055)
Air Density, kg/m^3	0.0938 kg/m^3	0.0082 kg/m^3
Static Temperature, K	216.67	237.2
Missile Velocity, m/sec	1475.0	1543.3
Angle of Attack, deg	0.0	0.0
Yaw Angle, deg	0.0	0.0
Molecular Weight	28.967	28.967
Ratio of Specific Heats	1.4	1.4

Table 2. Jet Interaction CFD Cases

Case No.	Time Integration	Jet Flow	Mach No.	Altitude kft (km)
1	Steady State	Off	5	64.5 (19.7)
2	Steady State	On	5	64.5 (19.7)
3	Transient	Jet Turning On	5	64.5 (19.7)
4	Transient	Jet Turning Off	5	64.5 (19.7)
5	Steady State	Off	5	115.0 (35.1)
6	Steady State	On	5	115.0 (35.1)
7	Transient	Jet Turning On	5	115.0 (35.1)
8	Transient	Jet Turning Off	5	115.0 (35.1)

Geometry and Computational Grid

The generic interceptor missile geometry was specified as a relatively long and slender configuration (L/D = 14.1) equipped with fixed dorsal and tail fins. The divert thruster nozzle exit was positioned flush with the missile surface between the dorsal fins at the center of gravity of the missile. The total length of the interceptor missile was specified as 195.74 in., which is equivalent to 14.5 calibers. One caliber is equivalent to one missile diameter, specified as 13.5 in. (34.3 cm). The nose geometry was modeled as a 2 caliber tangent ogive with a 0.33-in. (0.84 cm) radius spherical nose cap. The afterbody section is a 12.5-caliber cylinder. Very thin dorsal

and tail fins are rectangular in cross section and symmetrically positioned around the body at 45 and 135 deg from the symmetry plane. The dorsal fins have a 5-caliber chord and a 0.5-caliber span with the leading edge located 5 calibers from the nose tip. The tail fins have a 1-caliber chord and a 0.5-caliber span, with the leading edge located 13.5 calibers form the nose tip. The circular divert jet thrust chamber exit slot is flush to the missile body at 90 degrees. The exit slot diameter is 2.964 in. (7.53 cm). As shown in Fig. 1, the center of the exit slot is located on the interceptor missile body 6 calibers form the missile nose tip in the vehicle symmetry plane between the dorsal fins.

A computational grid was constructed for this geometry, including the interceptor missile and the internal thrust chamber of the divert thruster. The grid consists of 13 blocked meshes (approximately 2.6 million grid points) for the low-altitude cases and 14 blocked meshes (approximately 3 million grid points) for the high-altitude cases. An additional mesh was required for the high-altitude cases to completely capture the relatively larger underexpanded jet plume that occurs at the higher altitude, lower ambient pressure environment. The computational surface grid for the interceptor missile is presented in Fig. 2. A lateral control jet, also known as a divert control jet, is located at the missile center of gravity between the dorsal fins. The jet thrust is produced by a convergent-divergent

Fig. 2. Surface grid.

nozzle having supersonic exit conditions. The nominal exit Mach number is 3.0. An enlargement of the grid near the divert jet slot location on the missile surface is shown in Fig. 3. A very high grid density was constructed in the region upstream of the divert jet exit to obtain spatial details of the flow gradients in this complex JI region. A pitch plane-of-symmetry was assumed for all cases. The volume grid for the free-stream computational domain including all blocked meshes, is shown in Fig. 4. The divert jet thruster internal flow field was computed using the grid shown in Fig. 5. Grid points were packed near the nozzle walls to capture viscous effects. The thruster flow field was simulated from specified total conditions in the chamber, assuming thermally perfect, $\gamma = 1.4$ flow. This enabled the computations to capture the transient effects of the jet startup and account for the jet boundary layer and divergence at the exit plane.

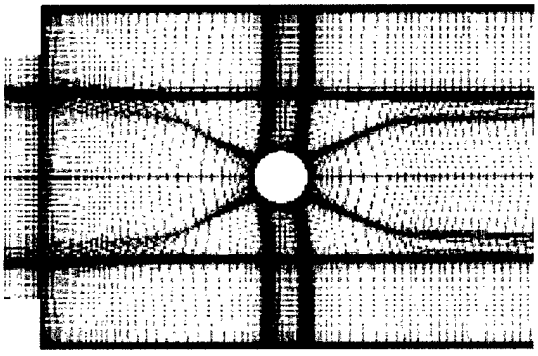

Fig. 3. Closeup view of surface grid around nozzle exit.

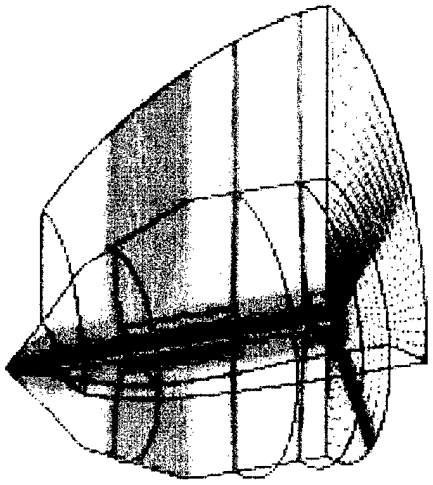

Fig. 4. Volume grid with high-altitude auxiliary grid.

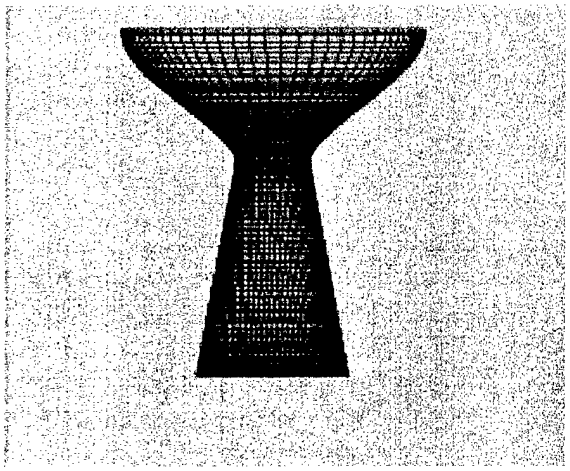

Fig. 5. Volume grid for lateral thruster.

Analysis

The General Propulsion Analysis Chemical Kinetic and Two-Phase, GPACT[3] was applied exclusively to simulate the complex at each condition. GPACT solves the integral form of the three-dimensional, time-dependent, Reynolds-averaged, full, compressible Navier-Stokes equations. GPACT is capable of solving subsets of these equations, including two-dimensional and axisymmetric equations. GPACT includes an optional multizone capability, which was applied in this study. The algorithm employs a shock-capturing solution scheme. This methodology is fully conservative because of the consistent manner in which properties such as computational cell volumes, surface areas, and numerical-flux functions are evaluated. The flow solver contains thermodynamic models and chemistry models. High-temperature effects such as vibrational relaxation and preferential dissociation can be included in the calculations. For this investigation, a thermally perfect gas was assumed. Several turbulence models are provided as user-selected options. The turbulence models include the two-layer algebraic model of Baldwin and Lomax, and fully coupled, two-equation k-ε models. An approximation accounting for turbulence-chemistry interacts is also available. The current study uses Van-Leer flux splitting, assumes the flow medium is a thermally ideal gas (γ = 1.4), and a k-ε model. Forces and moments on the missile body were obtained by integrating the surface pressures and viscous shear stresses over the entire surface of the missile. The effects of the interceptor base entrainment and associated forces were not evaluated. Divert jet thrust was obtained by integrating the calculated flux across the nozzle exit diameter of the jet.

Results and Discussion

The GPACT model provided converged flow-field solutions for all cases considered in the numerical investigation. Computational times for converged steady-state solutions ranged from 100-150 CPU hours on a Hewlett Packard SPP-2000 Exemplar computer using eight processors. Less CPU time was required for solutions obtained when the divert thruster was not operating. The transient computations were executed in time-accurate mode and required considerably longer CPU times. Additionally, transient CFD analyses cannot take advantage of convergence acceleration techniques. The transient computations required 20-40 CPU hours to integrate over 1 msec of physical time, depending on the time step and grid resolution. Initially, a time step of 0.2 μsec was used for the transient solutions. This value was increased in a stepwise fashion to 0.5 μsec as the computation proceeded. To assure an eventual steady-state condition, the transient methodology was continued to 14 μsec.

Free-stream conditions were specified on the far-field boundaries, and viscous no-slip assumptions were specified on all missile surfaces, including the divert jet thrust chamber walls. The thrust chamber wall boundary conditions specified for the divert nozzle inflow depended on the whether the thruster jet was operational. In the jet-off case, the nozzle inflow boundary was replaced with a slip wall, otherwise; a subsonic inflow boundary condition was used for the jet-on simulations. The divert thruster stagnation conditions (P_{oj} = 2590 psia and T_{oj} = 4100°R) were specified for the jet subsonic inflow boundary condition. Outflow boundary conditions equal to the free-stream ambient conditions were specified for the downstream boundary. For those simulations where the divert jet was turned off, the empty thrust chamber cavity, embedded within the interceptor surface, was included in the computational domain. The interceptor missile base aerodynamic effects were not computed; therefore, the force and moment contributions of the base region are neglected.

Flow-field results from the steady-state, jet-on calculation are shown in Fig. 6. Mach number contours at radial cross section are displayed at three axial locations flow corresponding to axial positions on the missile body: (1) just downstream of the divert jet, (2) the end of the dorsal fins, and (3) the end of the missile. The behavior of the under-expanded divert jet is indicated by the rapid divergence of the jet exhaust in the first cross section. Effects of the divert jet and free-stream interactions are noticeable at the downstream locations. Note the high-pressure interaction region impinging on the fins. This integrity of flow-field results in high gradient regions, such as the JI zones, is strongly dependent on the computational grid. Including the divert thrust chamber in the calculation, all the effects of the jet boundary layer are simulated.

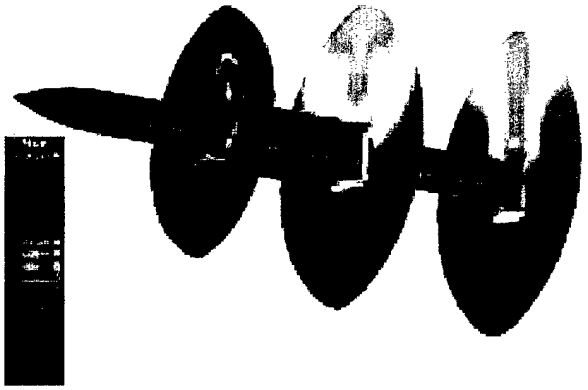

Fig. 6. Mach number contours for 64.5-kft altitude, jet-on case.

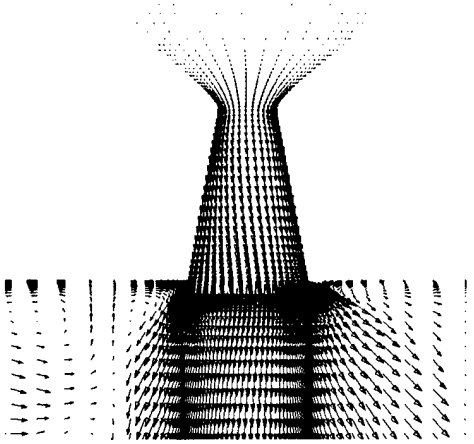

Fig. 7. Velocity vectors for 64.5-kft altitude, jet on case.

Since the divert jet operates in an underexpanded mode at both altitude conditions, the flow at the nozzle exit plane is supersonic (approximately Mach number 3.0). Under these conditions, the internal thrust chamber flow-field conditions are independent of the free stream, resulting in identical steady-state internal thrust chamber flow fields at both altitudes. However, the thrust at the higher altitude is expected to be larger because of the smaller ambient force term at the nozzle exit. Computed velocity vectors from the jet-on steady-state solution, including the thrust chamber and immediate free-stream interaction regions for the lower altitude (64.5 kft) Mach number 5 free-stream conditions are shown in Fig. 7. The large circulation bubble upstream created by the free-stream interaction with the divert jet plume is evident in the region upstream of the divert nozzle exit slot. A secondary separation region is also apparent. These recirculation zones create a high-pressure region and an associated force on the missile surface. The force exerted by the recirculation effect magnifies the divert jet's aerodynamic force, and also influences the moment about the center of gravity of the interceptor missile. As indicated on Fig. 7, the interaction on the downstream side of the divert jet creates an expansion region. Figure 8 shows a comparison of 64.5- and 115-kft Mach number contours. The lower ambient pressure at the high altitude produces a significantly larger jet plume and separation region compared to the lower-altitude results.

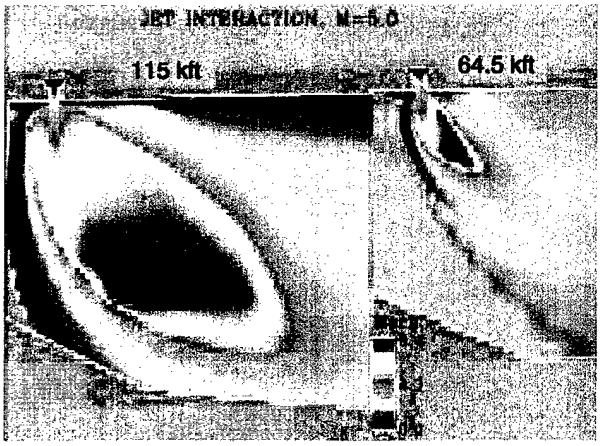

Fig. 8. Jet interation Mach No. contours-comparison of 64.5- and 115-kft.

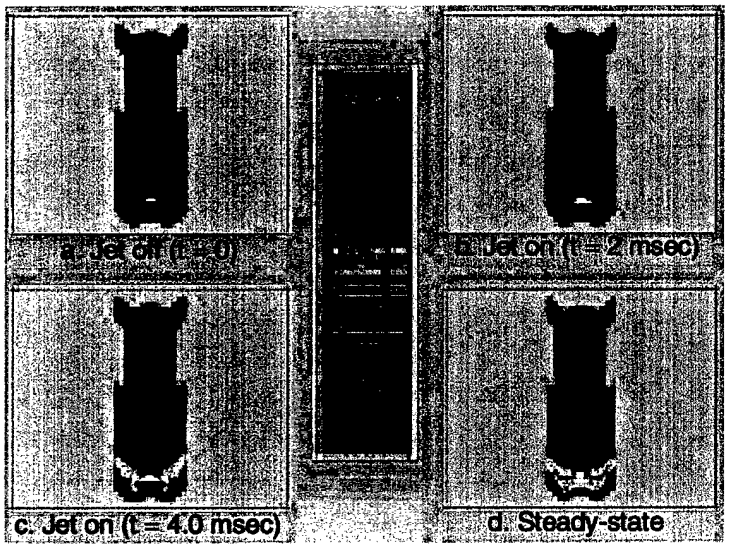

Fig. 9. Surface pressure at 64.5-ktf altitude, jet turning on case.

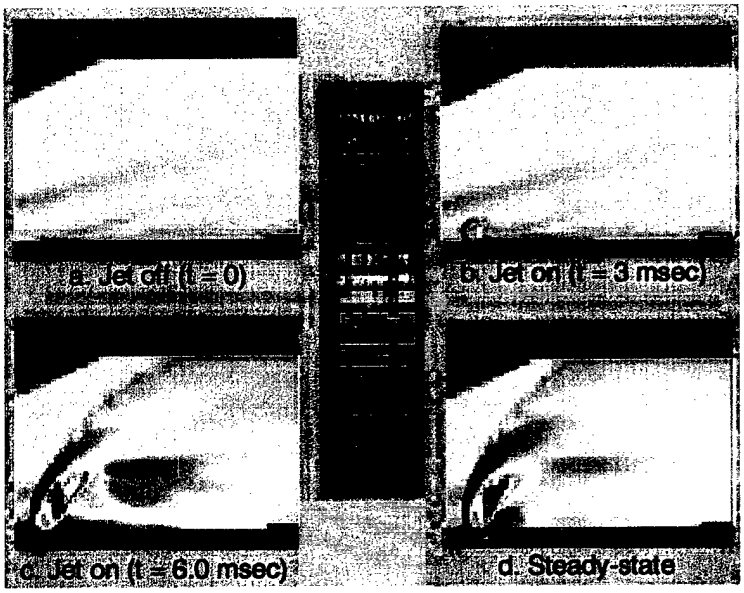

Fig. 10. Mach number contours for 64.5-ktf altitude, jet turning on case.

Figures 9-16 are the results of the transient JI solution at the 64.5-kft altitude condition showing the effects of the divert jet startup process. Several transient time slices are shown culminating in steady-state flow conditions at approximately 6 μsec. Figure 9 depicts the transient time slices of calculated static pressure on the surface of the interceptor vehicle from initiation of the jet flow at time = 0.0 to established steady-state flow at 8 μsec. Note the high-pressure interaction region impinging on the fins at 3.0 seconds. Consequences of this impingement will be observed in subsequent force analysis. Figure 10 includes corresponding Mach number contours in the free-stream and JI region symmetry plane covering the same time span as the flow develops. Steady-state Mach number contours are displayed at 8.0 μsec. These results clearly shown the development of JI shock and the associated high surface pressures and low Mach numbers in the recirculation zone upstream of the divert jet slot. The downstream expansion regions are characterized by supersonic flow and decreasing pressure. It is clear that Mach number contours on the symmetry plane are shown in Fig. 10 over the period of the jet turning on. A small disturbance can be seen at t = 0, caused by the presence of the nozzle cavity with no flow.

The surface integrated normal force and pitching moments calculated for the transient jet startup process (64.5 kft) are shown in Figs. 11 and 12, respectively. At t = 0, the jet is turned on and the force rises abruptly due to the jet force alone (~920 N). The exerted force continues to rise as the high-pressure recirculation region develops and spans increasing areas on the cylindrical missile body. The enhanced transient effect begins at approximately 2.6 seconds and occurs over a 1.2-μsec burst, creating normal body forces in excess of 3300 N at the maximum point. A steady-state condition is established near 6 μsec The steady-state force is approximately 1750 N and is greater than the magnitude of the jet force alone (920 N). The pitching moment (computed about the center of the divert jet) quickly rises to a value of 550 N-m as the jet is turned on, and then appears to remain steady over the period from 0-2.8 msec. The pitching moment then rises to a value approaching 2800 N-m over the 4-sec interval from 3-6.8 μsec. At

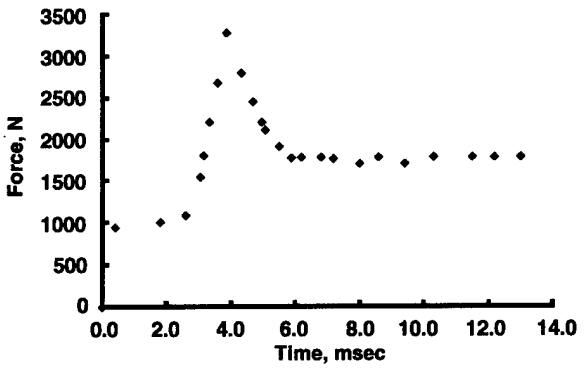

Fig. 11. Integrated normal force for jet turning on at 64.5 kft.

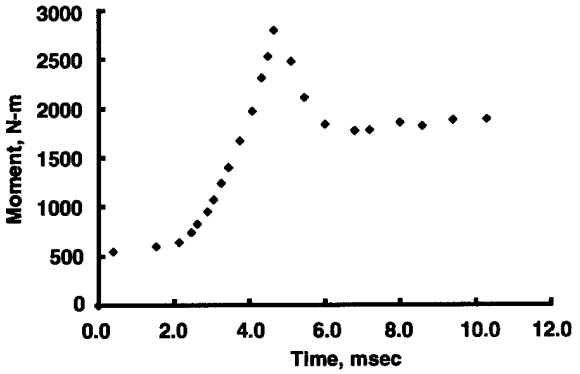

Fig. 12. Integrated pitching moment for jet turning on at 64.5 kft.

approximately 3.8 msec, the jet interaction region impinges on the dorsal fins in an abrupt manner with a force centered at the axial location of the jet. This is evident, as there is an abrupt change in moment with little change in force. After 4.0 msec, the high-pressure region established in front of the divert jet continues to travel upstream, causing a slight drop in surface pressure as the moving shocks begin to settle down and become more stationary and oblique to the oncoming free-stream flow. This causes a net decrease in the magnification force caused by the separation region acting on the missile. However, the resulting steady-state force (1750 N) is greater than double the force value computed for the divert jet alone (920 N).

Figures 13 and 14 show the integrated force and moment for the jet shutdown process at the 64.5-kft conditions. Time equal to 0.0 corresponds to when the thruster jet flow is extinguished. The force immediately begins to decrease as the jet shuts down. The interaction force appears to remain steady for 1.1 msec as the flow field adjusts to the new condition. The moment also appears to experience a delayed response to the jet shutdown, and begins to decrease after a period of approximately 1.5 msec. The final steady-state force equal to approximately 80 N and moment, equal to 120 N-m, are the result of the steady free steam flow. The normal force and pitching moment over a complete cycle, from jet start to shutdown at 64.5 kft, are shown in Figs. 15-16, respectively.

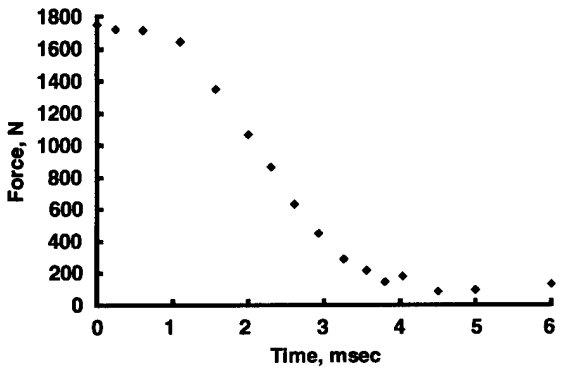

Fig. 13. Integrated normal force for jet turning off at 64.5 kft.

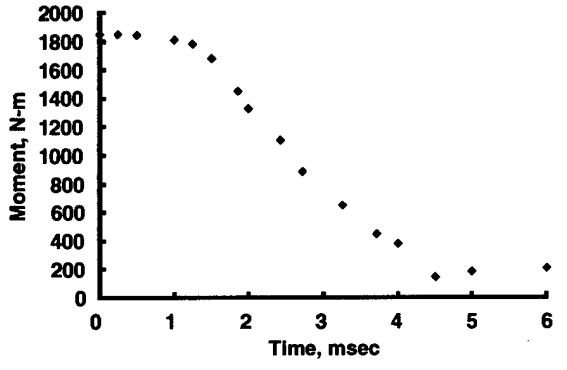

Fig. 14. Integrated pitching moment for jet turning off at 64.5 kft.

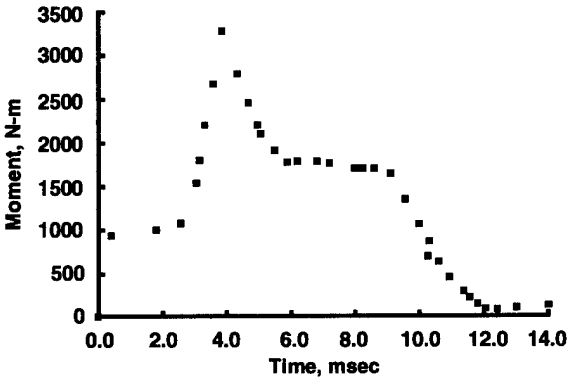

Fig. 15. Integrated normal forces from start to shutdown at 64.5 kft.

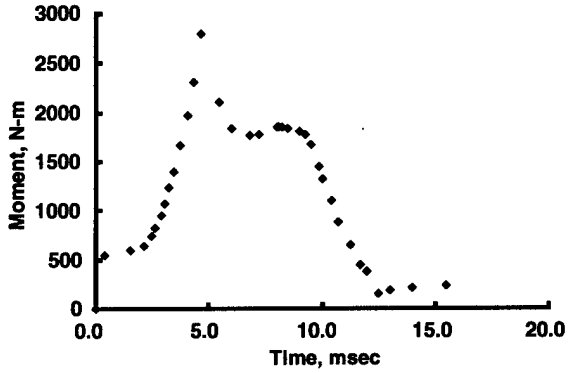

Fig. 16. Integrated pitching moment time trace from start to steady-state shutdown.

Corresponding results for the transient high-altitude solutions are shown in Figs. 17-21. The results have very similar trends when contrasted with the low-altitude results. Steady-state velocity vectors for the jet-on calculation, showing the divert jet thrust chamber and immediate free-stream regime, is shown in Fig. 17. Since the same jet conditions were used for this higher-altitude case, the divert jet nozzle is even more underexpanded at this higher altitude condition, resulting in a larger exhaust plume and deeper jet penetration into the free stream. The higher altitude case exhibits a larger separation region because of the

reduced momentum of the free stream, providing conditions that are more favorable for separation. Comparison of higher altitude at 115 kft with lower altitude at 64.5 kft are shown in Fig. 8. Note that although the separation region is increased at this altitude, the resulting pressure increase on the missile body is lower when compared with the lower altitude case. As will be shown in subsequent force profiles, the lower pressures in the separation zone (compared with the 64.5-kft solution) results in a decreased force magnification effect.

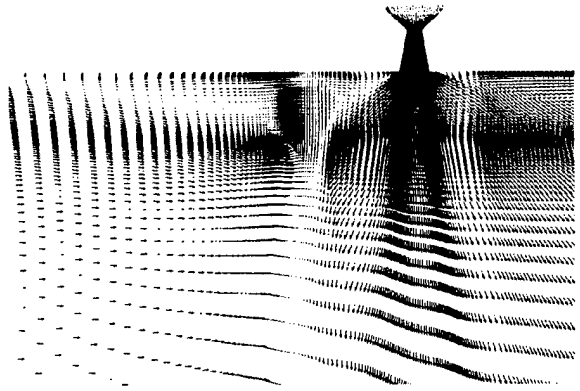

Fig. 17. Velocity vectors for 115-kft altitude, jet on case.

Figures 18 and 19 show the transient jet startup process for the high-altitude case. Static missile surface pressures are shown in Fig. 18 at time slices corresponding to initial startup until steady-state flow is reached at approximately 8.0 μsec. The plume is bigger at this higher altitude condition, and the JI region impinges on the dorsal fins earlier. However, because of the lower pressure environment, it is expected that the corresponding impingement force will be lower. Free-stream Mach number contours in the horizontal symmetry plane of the divert nozzle over the same time span are shown in Fig. 19. Larger plume expansion, deep divert jet penetration into the free stream, and very large recirculation regions are evident in these results.

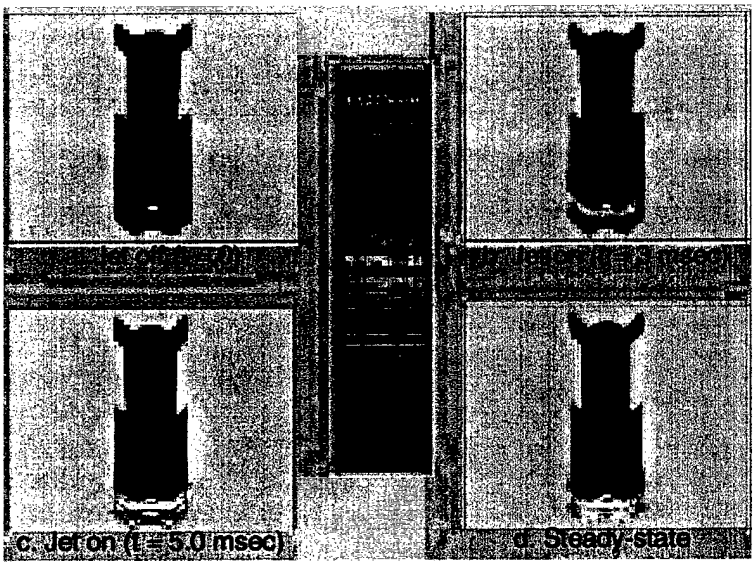

Fig. 18. Surface pressure for 115-kft altitude, jet turning on case.

The surface integrated force and moment values for the jet startup transient process at the higher altitude (115 kft) conditions are shown in Figs. 20-21. These plots exhibit similar trends to the lower altitude results, but are less abrupt. The transient spike occurs earlier in the startup process (3.5 msec vs. 3.8 msec) and is more gradual compared with the lower-altitude solution. The JI impingement on the dorsal fins occurred earlier at this condition; the transient burst is predicted to occur earlier. Recall that the time corresponding to the peak force was correlated with the impingement of the JI region on the missile dorsal fines at the lower altitude condition.

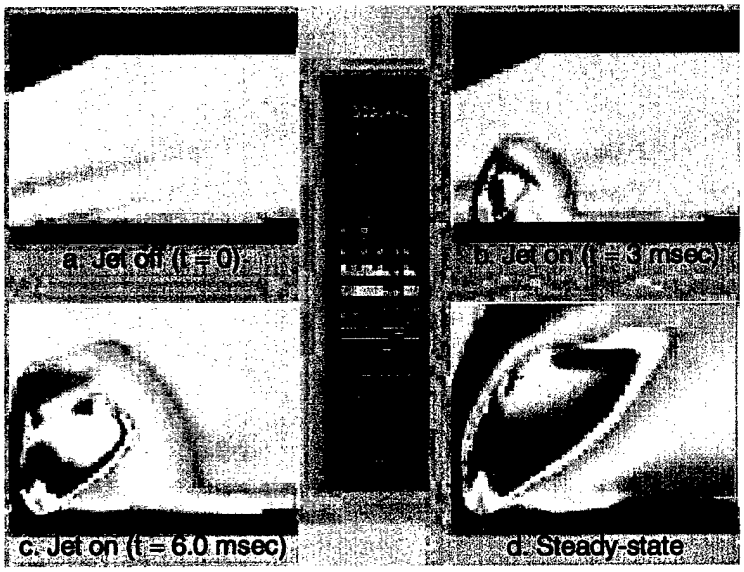

Fig. 19. Mach number contours for 115-kft altitude, jet turning on case.

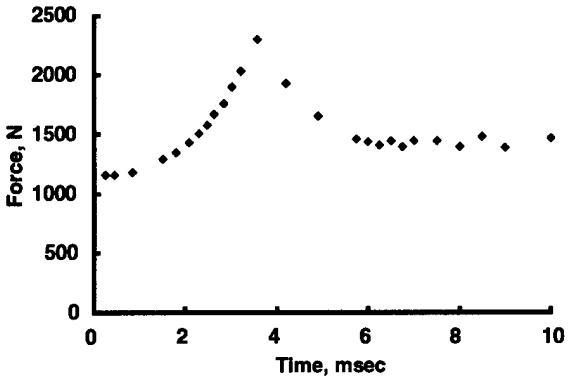

Fig. 20. Integrated normal force for jet turning on at 115 kft.

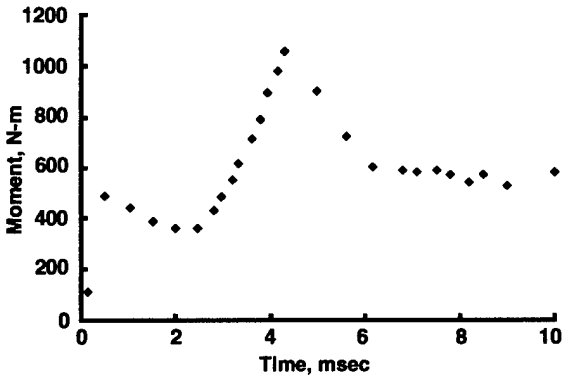

Fig. 21. Integrated pitching moment for jet turning on at 115-kft.

The peak transient interaction force (~2200 N) at the higher-altitude conditions is considerably less than the lower-altitude peak force (3300 N). The is attributed to the lower pressures at the higher altitude. The moment transient increase is very gradual, lagging the force trend, as was evident in the lower-altitude results.

Force and moment profiles for the jet shutdown transient at 115 kft altitude is shown in Figs. 22 and 23, respectively. These results are very similar to the shutdown behavior at the lower altitude. The steady-state value at the end of the shutdown transient is lower because of the lower pressure in the free stream. These results indicate that shorter times are required to reach steady-state conditions at the high-altitude condition. This could be influenced by the very large jet penetration and recirculation regions that result at higher altitudes. The normal force andpitching moment over a complete cycle from jet start to shutdown at 115 kft are shown in Figs. 24 and 25, respectively.

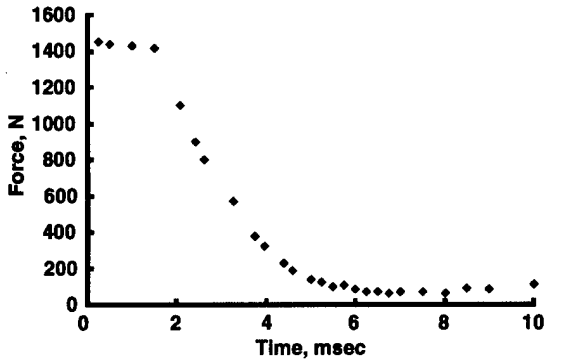

Fig. 22. Integrated normal force for jet turning off at 115-kft.

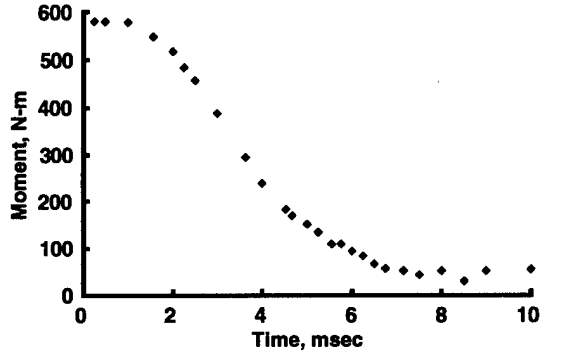

Fig. 23. Integrated pitching moment for jet turning off at 115 kft.

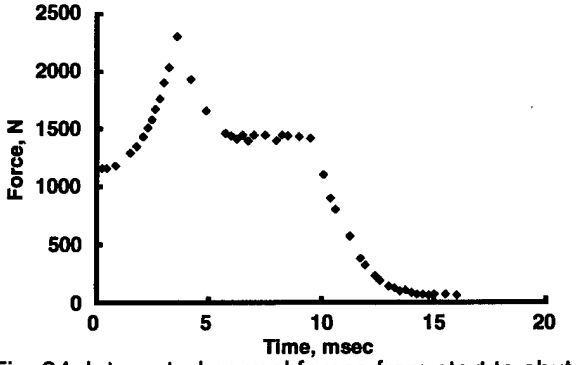

Fig. 24. Integrated normal forces from start to shutdown at 115 kft.

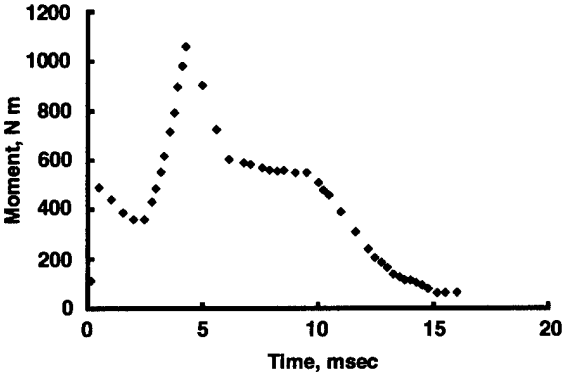

Fig. 25. Integrated pitching moment from start to shutdown at 115 kft.

Summary

Transient jet interaction computations were completed to assess the transient effects of a reaction control thruster on the free-stream flow field,and normal forces and pitching moments on a generic interceptor missile. The results indicate a strong transient effect that must be considered when designing control algorithms for pulsed-jet reaction control systems with short pulse times. The transient interaction at low altitudes on this type of finned geometry causes short durations of high force that diminish at higher altitudes. This very strong jolt is caused by the high-pressure region in front of the jet exhaust gasses as it abruptly impacts the dorsal fins. These pressures are higher than the steady pressures because of moving shocks. The transient effects seem to last approximately 3-6 msec at both high and low altitudes before the force begins to steady out. The jet shutdown case required less time to reach steady-state conditions than the jet startup process.

This investigation demonstrates the utility of state-of-the-art CFD tools to address issues pertaining to the most complex flow interactions of interest in the propulsion arena. While these solutions require considerable CPU resources, they provide an economical means to supplement interceptor design and testing and have the potential to save development and testing resources. CFD solutions such as those presented in this study can be applied to maximize the test matrices and to evaluate paper designs and identify potential problem area prior to production. The CFD flow fields can be analyzed to gain insight into the force amplication phenomena and to understand the transient behavior. The flow-field details calculated and visualized in this study cannot be measured at the harsh conditions using modern flow visualization techniques. Additional CFD studies investigating the effects of chemistry in the interaction region are needed to complete the CFD feasibility demonstration.

References

1. Srivastava, B., "Lateral Jet Control of a Supersonic Missile: CFD Predictions and Comparison to Force and Moment Measurements," AIAA 97-0639, January 1997.

2. Ebrahimi, H. B., "Validation Database for Propulsion Computation Fluid Dynamics," *Journal of Spacecraft and Rockets*, Vol. 34, Oct. 1997, pp. 642-650.

3. Ebrahimi, H. B. and Kawasaki, Alan, "Numerical Investigation of Exhaust Plume Radiative Transfer Phenomena," AIAA 98-3623, July 1998.